water

MDPI

Article

Study of the Photocatalytic Activity of TiO_2 and Fe^{2+} in the Activation of Peroxymonosulfate

Rodrigo González-Quiles, Juan Manuel de Andrés and Jorge Rodríguez-Chueca *

Department of Industrial Chemical & Environmental Engineering, Escuela Técnica Superior de Ingenieros Industriales, Universidad Politécnica de Madrid, Calle José Gutiérrez Abascal 2, 28006 Madrid, Spain; quilesrodrigo@gmail.com (R.G.-Q.); juanmanuel.deandres@upm.es (J.M.d.A.)

* Correspondence: jorge.rodriguez.chueca@upm.es; Tel.: +34-9106-77334

Abstract: The increase in world population and human activities are leading to an increase in water stress in many regions of the planet, coupled with a decrease in the quality of water bodies. Advanced oxidation processes have demonstrated great potential for the reduction of almost any organic pollutant; however, it is necessary to intensify this type of treatment in order to reduce contact times and to reach a greater number of pollutants. The generation of sulfate radicals by activation of peroxymonosulfate (PMS) by divalent iron (Fe^{2+}) and/or titanium dioxide (TiO_2) were statistically studied to understand the role of these compounds as activators, using methylene blue as target pollutant because of its ease of handling and analysis. A factorial experimental design was used to study the influence of different variables (PMS, Fe^{2+}, and TiO_2) in the presence of UV-A or UV-C. There were relevant differences in the discoloration of methylene blue when analyzing the size of the effects and significance of the experiments, when UV-A or UV-C was used, being faster with UV-C. For instance, total discoloration of methylene blue was reached after 60 min with the system PMS/UV-C, while after 90 min only the 59% of methylene blue disappeared in presence of PMS/UV-A. Both Fe^{2+} and TiO_2 in combination with PMS and UV increased the discoloration effect. So, in the presence of Fe^{2+}, total discoloration of methylene blue was observed after 30 min in presence of UV-A, while this yield was reached in 7.5 min under UV-C. In the case of PMS/TiO_2, it required 60 min under UV-A radiation to totally remove methylene blue, and around 15 min with UV-C. Statistically, the three variables were observed to have the main effect in combination with UV. Furthermore, the PMS/Fe^{2+} system has a significant interaction with UV-A and UV-C radiation, while the interaction of PMS/TiO_2 was significant under UV-A, but with a negative effect under UV-C, or in other words the high elimination rates observed are achieved by the oxidation potential of UV-C, and the effect of PMS and TiO_2 by itself.

Keywords: heterogeneous photocatalysis; peroxymonosulfate; sulfate radicals; TiO_2; UV radiation

Citation: González-Quiles, R.; de Andrés, J.M.; Rodríguez-Chueca, J. Study of the Photocatalytic Activity of TiO_2 and Fe^{2+} in the Activation of Peroxymonosulfate. *Water* **2021**, *13*, 2860. https://doi.org/10.3390/w13202860

Academic Editor: Chengyun Zhou

Received: 24 August 2021
Accepted: 8 October 2021
Published: 13 October 2021

1. Introduction

Advanced oxidation processes (AOP) have been shown to be efficient treatments for the removal of organic and biological pollutants in water [1–7], and are especially useful for the degradation of recalcitrant organic pollutants that cannot be removed by conventional methods, such as dyes or other persistent contaminants [8–11]. Sulfate radical-based advanced oxidation processes (SR-AOPs) are emerging alternatives to hydroxyl radical-based AOPs (HR-AOPs). Both AOPs are based on the production of free radical species, with a high redox potential of 2.5–3.1 V (25 °C) and 2.80 V (25 °C) for sulfate and hydroxyl radicals, respectively [12–14]. Furthermore, SR-AOPs have some advantages, such as the lack of toxicity of persulfate salts, the ease of handling and storage, and a very low pH-dependent activity [12]. However, the generation of sulfate radicals requires the activation of persulfate salts such as potassium peroxymonosulfate (HSO_5^-; PMS). The main activation mechanisms reported are thermal, UV-assisted, or catalyzed by a metal or a metal oxide [12–18].

The use of UV radiation as an activator is widely reported in the literature [13,19–22]. It has been demonstrated that PMS are effectively activated at wavelengths around 254 nm (UV-C) [13,22]. However, the activation of these salts with UV-A and UV-visible radiation has also been reported [12,19,21,23,24]. In both cases, the generation of hydroxyl and sulfate radicals is a consequence of the breakage of the peroxo bond (O-O). However, as previously mentioned, the decomposition kinetic of PMS will depend on the kind of UV radiation used. The more energetic radiation (as it is the case for UV-C), the higher kinetic [12,13].

Although PMS activation by Fe^{2+} has been widely reported, as well as other iron species and even other types of transition metals [1,25–29], the generation of sulfate radicals by PMS activation with photocatalysts such as TiO_2 is still poorly explored [30–34]. It seems that a synergistic effect occurs when PMS and TiO_2 are coupled, and the most feasible mechanism is the decomposition of PMS by TiO_2, while photolysis of PMS can enhance the reactivity of TiO_2 and inhibit the recombination of the electron–hole pair by trapping photoinduced electrons [35,36]. To the best of our knowledge, there are no references in the literature that compare PMS activation by TiO_2 and Fe^{2+} to suggest which catalyst may be preferable. Since Fe^{2+} and TiO_2 are commonly used with UV spectra, analyzing the magnitude of the effects of these variables on the activation of PMS may be considered highly relevant, not only to know how they affect the reaction time, but also to know how they interact with each other.

Normally, iron activation is commonly used in conjunction with UV radiation in order to promote a quick photoreduction of Fe^{3+} generated in Fe^{2+} to continue catalyzing the generation of free radicals by PMS decomposition. Additionally, TiO_2 is one of the most reported photocatalysts [34]. For that reason, the study of the influence variables in the activation of PMS by Fe^{2+} and TiO_2 were carried out in the presence of UV-C and UV-A radiation.

The main purpose of this research was to statistically compare the effect of a set of variables (Fe^{2+}, TiO_2, and UV radiation) on the activation of PMS, as well as to study their possible interactions. Therefore, a full 2^k factorial design was used to check changes in the response (PMS activation) because of changes in the catalyst concentration and type of UV radiation. Thus, the design of experiment was repeated twice, as it was also sought to observe the effect caused by UV-A and UV-C radiation over the activation mechanisms. An ANOVA was performed for both sets of experiments to determine whether the effects of the factors and their interactions were statistically significant in both cases. In addition, to estimate the magnitude of the effects, a *t*-test was performed in both cases.

2. Materials and Methods

2.1. Chemical Reagents

The study of the influence of the selected variables in PMS activation was investigated in the discoloration of methylene blue. Methylene blue (MB; $C_{16}H_{18}ClN_3S$; M_w = 319.8 g/mol) was provided from Scharlau (Spain) and used as received, without further purification. The physicochemical features of MB, such as high solubility, stability, and glow, and low biodegradability and toxicity, make it ideal for study. MB concentrations throughout the experiments were 10 ppm [37,38]. The UV-visible spectrum of MB consists of a main characteristic absorption band at 660 nm. Discoloration treatments were carried out by activation of potassium peroxymonosulfate ($KHSO_5 \cdot 0.5KHSO_4 \cdot 0.5K_2SO_4$, PMS, Merck) with iron sulfate heptahydrate ($FeSO_4 \cdot 7H_2O$, Panreac) and titanium dioxide (Evonik Aeroxide® P25). In addition, HCl and NaOH (Scharlau) were used to adjust the pH at 7.

2.2. Experimental Setup

The experiments were carried out in a 1 L rectangular batch reactor, using a 200 mL volume of MB solution sample, with 1 cm depth, and 15 cm between the UV lamp and the MB solution. UV-driven experiments were performed with UV-A or UV-C depending on the experiment in progress. UV-A radiation was provided from the top by a Philips TL 6 W (maximum emission peak at 365 nm), while UV-C radiation came from a Philips

6W TUV lamp (maximum emission peak at 254 nm). The MB solution was continuously stirred throughout the experiments.

2.3. Experimental Procedure

Samples were prepared by dissolving 10 mg/L of MB in deionized water. Then, different doses of reagents were added according to the corresponding experiment (PMS 0–500 mg/L; TiO_2 0–500 mg/L; Fe^{2+} 0–0.5 mM). These concentrations were used according to previous research and literature where the molar ratio was reported by some authors, when using Fe^{2+} and PMS, was 1:1, or less; when experiments used additional UV-A radiation, more Fe (II) than that ratio would likely cause a decrease in PMS activation performance [39–43]. Reagents were added directly to the reactor at the beginning of each experiment when the ultraviolet radiation was switched on. Treatments were applied for a maximum of 120 min at a neutral pH (pH = 7).

Samples of the MB solution were collected at periodic intervals during each experimental run and analyzed using a Mettler Toledo UV5 spectrophotometer. The discoloration of MB was obtained by measuring the absorbance at the maximum wavelength (λ_{max} = 660 nm). The pH of the samples was monitored using a pH Meter from XS Instruments (model PC 8).

2.4. Experimental Design

A two-level factorial design (2^k) was selected for the experimental design, in which each variable assumes two values or levels. This design was the most suitable for learning about the influence of variables on the process. The program used was the Windows version of MINITAB 18®.

The variables considered for these studies were: PMS concentration, Fe^{2+}, and TiO_2. A total of 34 experiments (16 + experiment of central points) were carried out for both UV-A and UV-C radiation. Replica central points served to evaluate the experimental error and the curvature of the evolution of a response factor, that is, whether or not the evolution of the response factor was linear within the experimental range studied [44]. The conditions in each experiment were modified using different combinations of the two selected levels (Table 1).

Table 1. Levels of selected variables.

Variable	Low Level, −1	Central Point	High Level, +1
[PMS] (mg/L)	0	250	500
[TiO_2] (mg/L)	0	250	500
[Fe^{2+}] (mg/L)	0	14	28

3. Results and Discussion

Table 2 shows the design matrix obtained with MINITAB® considering the concentration of PMS, TiO_2, and Fe^{2+} as variables. It includes the experimental conditions and the results obtained in each experiment run after 10 min of exposure to UV-A and UV-C radiation. The response factor used was the discoloration of the MB (expressed as %). In the following sections, the influence of each variable on the MB discoloration is discussed from a statistical point of view.

Table 2. Design matrix and methylene blue discoloration results obtained by UV-A and UV-C exposure.

Experimental	PMS (mg/L)	TiO_2 (mg/L)	Fe^{2+} (mg/L)	Discoloration (%)	
				UV-A	UV-C
1	0	0	28	1	9
2	250	250	14	72	48
3	0	500	0	1	61
4	500	500	0	62	96
5	0	0	0	0	7
6	500	500	28	100	100
7	500	500	28	100	100
8	500	0	0	21	54
9	0	0	28	1	18
10	0	500	28	27	85
11	500	500	0	58	99
12	0	500	28	21	84
13	0	0	0	0	7
14	500	0	28	63	100
15	500	0	28	63	100
16	0	500	0	8	45
17	500	0	0	20	38

3.1. Methylene Blue Discoloration by PMS/UV, TiO_2/UV and Fe^{2+}/UV as a Reference

Before analyzing PMS activation by TiO_2 or Fe^{2+}, the analysis of the effect of using each individual agent in combination with UV radiation should be evaluated. In this regard, Figure 1 shows the discoloration of MB after the combination of PMS/UV, TiO_2/UV, and Fe^{2+}/UV.

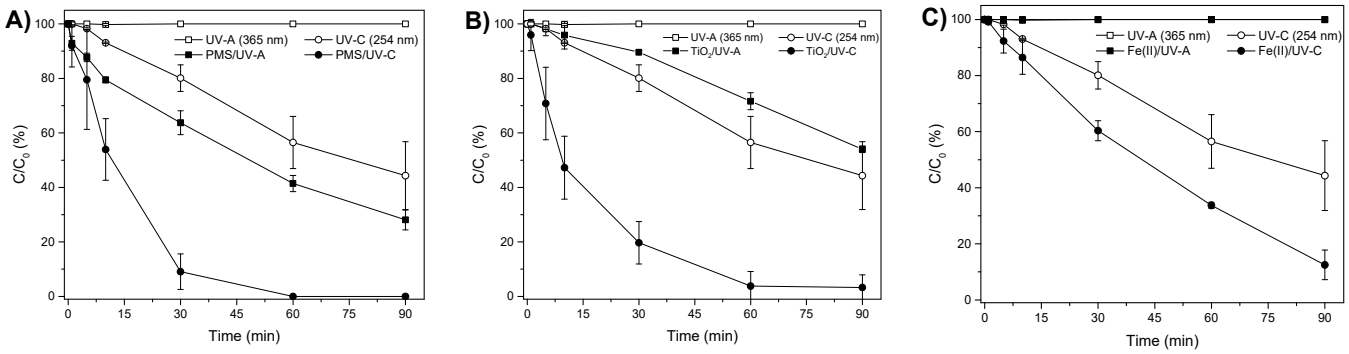

Figure 1. MB discoloration (%) with (**A**) 500 mg/L PMS; (**B**) 500 mg/L TiO_2; (**C**) 28 mg/L Fe^{2+}; using UV-A and UV-C radiation.

According to [45], the dissociation capacity of PMS in the presence of UV radiation ranged from 248 nm to 351 nm, and decreased as the wavelength increased, so the ability to generate sulfate radicals by PMS is conditioned by the type of UV radiation used. This fact can be clearly observed in Figure 1A, where the discoloration yields of MB combined with 500 mg/L of PMS were 59% and 100% after 60 min of exposure to UV-A and UV-C radiation, respectively. Although PMS requires prior activation to generate free radicals, its remarkable oxidation potential allows, even in the absence of radiation, the MB to be slightly reduced, namely by 6.5% in 120 min [30]. The removal performance caused by the activation of the PMS is higher under both UV spectra regarding the treatments that did not contain the reagent. Furthermore, it is observed how UV-C radiation removes MB by itself, without using PMS. Figure 1 shows that UV-A radiation alone does not reduce the concentration of methylene blue, which differs from the results found by Andrade et al. [46]. This discrepancy may be explained by the operating conditions used in this study, especially

the irradiance. Irradiance will be affected by the radiation power of the lamp used, the position of the lamp with the water sample, and the type of reactor that would affect the radiation distribution in the sample.

A similar result was observed in the exposure of TiO_2 to UV (Figure 1B). Although the valence band of TiO_2 is excited by both UV radiations, after 90 min of experiment the average removal yield when TiO_2 was used with UV-C radiation reached 97%, while 45% was reached in the presence of UV-A radiation. The TiO_2 valence band is capable of absorbing photons in the presence of electromagnetic radiation in the ranges below 390 nm [47], which represents two decontamination routes for this compound: (i) the reductive pathway, through the release of electrons that will reduce the concentration of MB; (ii) the oxidative pathway in the gaps of the valence band that absorb electrons from either the contaminating compound or from water, which will produce hydroxyl radicals capable of oxidizing MB. Besides, it is required to remark that according to Tichapondwa et al. [48], in the system TiO_2/UV-C to remove MB, 1.3% corresponds to photolysis, 7.4% to adsorption, and 81.4% to photocatalysis.

Figure 1C plots the discoloration of MB using the Fe^{2+}/UV system. As can be observed, the combination Fe^{2+} with UV-A radiation did not reduce the MB concentration. However, the use of Fe^{2+}/UV-C slightly increased the discoloration yield because when Fe^{2+} is subjected to UV radiation around 250 nm, it is capable of dissociating water molecules or those of any compound with which it interacts, following the reaction mechanism described in Equation (1) [49].

$$Fe(OH)^{2+} \xrightarrow{h\upsilon} Fe^{2+} + OH^{\bullet} \quad (1)$$

The effect of Fe^{2+} in the dark over MB was negligible (1.5% of removal) after 120 min (data not shown).

3.2. Methylene Blue Discoloration by the PMS/Fe^{2+}/UV System

Figure 2 shows the removal rates for the experiment using UV-A and UV-C radiation with PMS and Fe^{2+}. As can be observed, the use of Fe^{2+} to activate PMS increased the discoloration performance of MB compared with treatments without catalyst, as a consequence of the increase in the kinetics of sulfate radical generation [19–21,23,24]. Exposure to UV-C radiation increased the discoloration rate by 50% compared with the values obtained by UV-A, reducing the time required to achieve the total removal of MB at around 5 min.

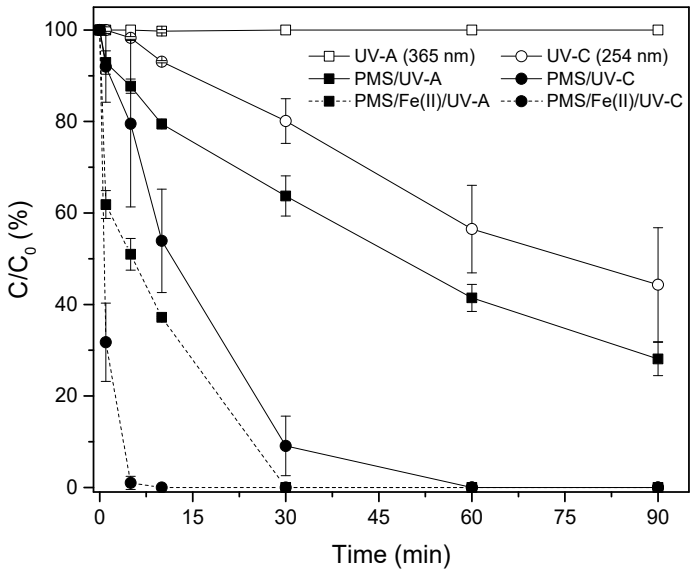

Figure 2. MB discoloration (%) through the PMS/Fe^{2+} system, under UV-A and UV-C radiation. [PMS] = 500 mg/L; [Fe^{2+}] = 28 mg/L.

The use of Fe^{2+} for PMS activation considerably increased the average discoloration performance of MB compared with treatments using only PMS (39% when using UV-A; and 51% when using UV-C). In both cases, the effects were higher than those found with UV/PMS alone, thus indicating a multiplicative effect of the divalent iron and PMS.

The results obtained were expected, while several studies describe the mechanisms by which divalent iron enhances the production of sulfate radicals [49,50]. However, it is important to consider that the mechanisms of radical production are multiple. The dissociation of PMS by Fe^{2+} follows the subsequent equations (Equations (2)–(7)).

$$Fe^{2+} + HSO_5^- \rightarrow Fe^{3+} + SO_4^{\bullet -} + OH^- \quad (2)$$

$$Fe^{3+} + HSO_5^- \rightarrow SO_5^{\bullet -} + Fe^{2+} + H^+ \quad (3)$$

$$Fe^{2+} + SO_4^- \rightarrow Fe^{3+} + SO_4^{2-} \quad (4)$$

$$HSO_5^- + SO_4^{\bullet -} \rightarrow SO_4^{2-} + SO_5^{\bullet -} + H^+ \quad (5)$$

$$HSO_5^- + H_2O \rightarrow SO_4^{2-} + 2HO^{\bullet} + H^+ \quad (6)$$

$$SO_5^{\bullet -} + 2H_2O \rightarrow SO_4^{2-} + 3HO^{\bullet} + H^+ \quad (7)$$

In the previous reactions, the production of sulfate radicals, which are the most desirable due to their high oxidation capacity, occurs due to the reaction of PMS with Fe^{2+}. However, a series of reactions are triggered that will result in the production of different types of radicals, such as sulfur pentoxide or hydroxyl, and some anions with less oxidation capacity. The increase in yield and speed in this treatment can be associated with the interaction of the contaminant with a wide variety of oxidizing compounds, and the regeneration of divalent iron by UV spectra [15,40,45].

Furthermore, it is necessary to consider that these reactions are influenced by the operation conditions and are not the only ones occurring. For example, the dissociation action exerted by UV-C radiation on water molecules and PMS, which will provide radicals to the media and reaction intermediates, enhancing or reducing the activity of Fe^{2+} to destroy pollutant molecules [13,51]. Other examples of reactions that occur in the media are those related to the oxidation of ferric compounds by the action of water that will provide hydroxyl radicals to the media [49]. Consequently, the decrease of the pollutant would occur not only by the oxidation caused by sulfate radicals, but also by a constant association and dissociation of molecules with iron due to photolysis of ferric compounds and regeneration of Fe^{2+}. However, this regeneration mechanism largely depends on the wavelength of the UV spectrum, since it increases when the radiation is above 300 nm. Therefore, it is possible to think that it occurs largely when subjected to UV-A, regarding UV-C, and possibly explaining the increase in the estimated effect, which was higher than that of UV-C.

3.3. Methylene Blue Discoloration by the PMS/TiO_2/UV System

As shown in Figure 3, the activation of PMS by the combination of 500 mg/L of TiO_2 and PMS increased the MB removal rates under both UV radiations. The catalyzed experiment subjected to UV-C radiation removed 97% of MB after 7.5 min (performance 60% higher than that obtained with PMS/UV-C). The test carried out with UV-A radiation required 60 min to reach the same removal efficiency.

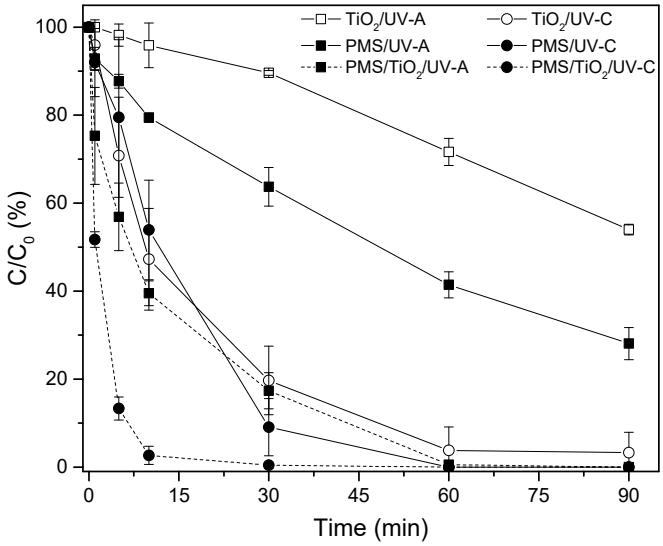

Figure 3. MB discoloration (%) through the PMS/TiO_2 system, under UV-A and UV-C radiation. [PMS] = 500 mg/L; [TiO_2] = 500 mg/L.

The photocatalysis of TiO_2 increased as the wavelength decreased from UV-A to UV-C, approximately 280 nm. Therefore, the absorption of photons and the subsequent release of electrons for the activation of PMS are possible routes of MB degradation, generating sulfate radicals, hydroxyl radicals, and anions with oxidative power. Nevertheless, other routes of degradation should be considered, such as holes in the valence band, which could produce hydroxyl radicals in contact with water [31,33].

3.4. Methylene Blue Discoloration by the PMS/TiO_2/Fe^{2+}/UV System

As shown in Figure 4, the addition of PMS, Fe^{2+}, and TiO_2 at concentrations of 500 mg/L, 0.5 mM, and 500 mg/L, respectively, increased the discoloration performance of MB compared with the individual combination of the reagents under the UV radiations studied. In the UV-C experiment, MB was completely removed after 1 min of the experiment, while an average removal of 81.5% was reached with UV-A radiation (Figure 4).

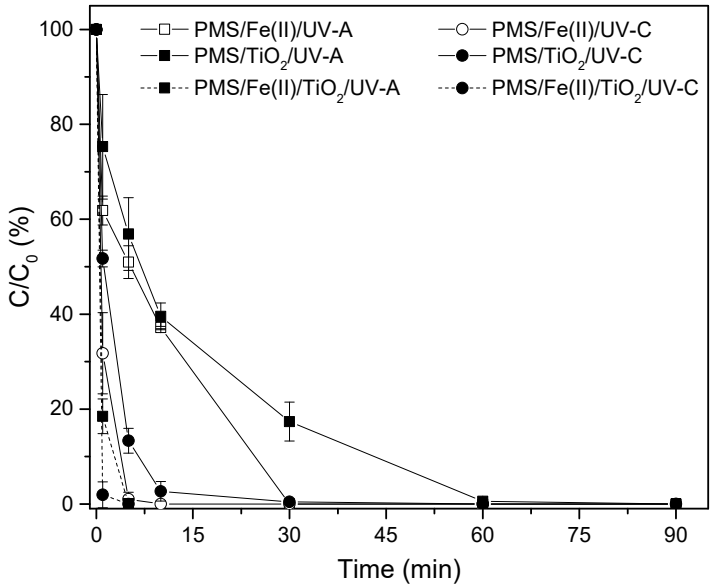

Figure 4. MB discoloration (%) through the PMS/Fe^{2+}/TiO_2 system, under UV-A and UV-C radiation. [PMS] = 500 mg/L; [Fe^{2+}] = 28 mg/L; [TiO_2] = 500 mg/L.

This high removal efficiency was expected since the routes of radical production are multiple. Additive effects are the possible way for radicals to be produced, increasing the removal performance of MB, considering that there is no evidence that multiplicative effects contributed to elimination yields. Possible additive routes are hydroxyl radicals created, either due to its reduction action by releasing electrons or by contributing to the production of radicals generated by the interaction with PMS.

3.5. Statistical Analysis of the Influence of Variables

Figure 5 plots the main effects for the three variables (PMS, TiO_2, and Fe^{2+}) on the response factor, the MB discoloration, in combination with UV-A (Figure 5A) and UV-C radiation (Figure 5B), after 10 min of reaction. It is clearly observed that these three variables have a main effect on the discoloration of MB, being higher with UV-C radiation, as previously shown in the discoloration kinetic plots. In the case of UV-A driven assays, the maximum effect is obtained with the central concentration point of the three variables, decreasing the effect with a higher concentration (Figure 5A). When using UV-C radiation, it can be observed that there are no significant differences in MB discoloration in terms of the main effect of the individual variables, obtaining similar yields with PMS or TiO_2, the effect using Fe^{2+} being slightly lower. The main effect is the average effect of every experiment containing one factor and its combinations, so that the main effects of Fe^{2+} similarities to the main effects of other factors can be explained by the catalysis that this compound exerts on PMS, but also by the effect caused by UV-C radiations by itself. The *p*-value of Fe^{2+} obtained when using exclusively Fe^{2+} exposed to both spectra (Table S1, Supplementary Material) shows that there is blue discoloration of MB occurring, also likely due to oxidation of ferric compounds in the water that could lead to the production of hydroxyl radicals when using UV radiation.

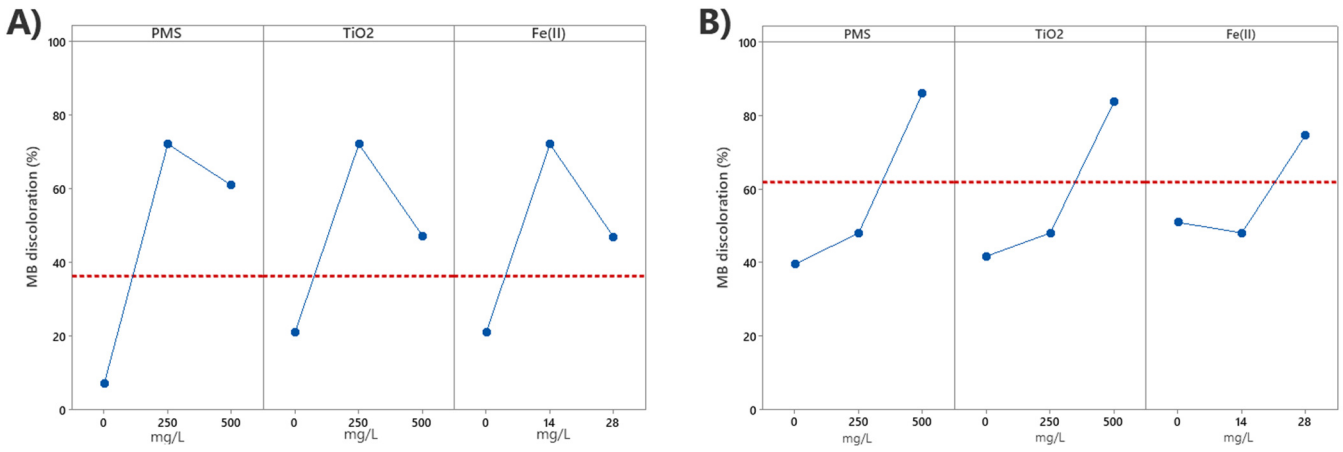

Figure 5. Main effects plot for MB discoloration using (**A**) UV-A radiation; (**B**) UV-C radiation.

Figure 6 shows the interaction between variables under UV-A and UV-C radiation (Figure 6A,B, respectively). Under UV-A radiation (Figure 6A), PMS interacts strongly with TiO_2 and Fe^{2+}; however, there are no interactions between TiO_2 and Fe^{2+} as the plotted lines are almost parallel. The interactions under UV-C are quite different (Figure 6B). Again, there is an interaction between PMS and TiO_2, and it can be considered a negative interaction because of the tendency of the lines to cross at some point. This negative interaction can be confirmed by numerical regression, where the standardized value of the effect is -0.16, meaning that high performance in discoloring MB is achieved by the addition effects of PMS by its own, plus the additive effect of TiO_2 by its own, and the effect exerted by UV-C, but also that the interaction of the three factors can reduce this additive effect of the three factors. Furthermore, there is a slight interaction between TiO_2 and Fe^{2+} and PMS and Fe^{2+}, but the lines are almost parallel and further statistical analysis is required to confirm the interactions and their significance. In the particular case of the PMS and Fe^{2+}

interaction when subjected to UV-C radiation, a complete degradation of MB was achieved before 10 min, so the interaction plots are underestimated when compared with the effect exerted by PMS on its own. Therefore, interaction plots at 5 min of the experiment were also obtained (Figure 7), showing that the interaction is higher than those experiments at 10 min, but slightly less than the UV-A radiation experiments.

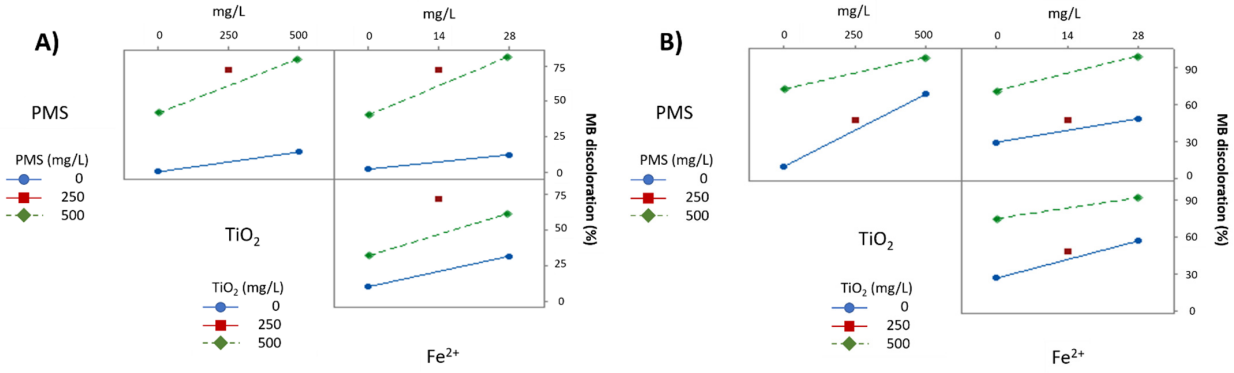

Figure 6. Interaction of variables plot under (**A**) UV-A radiation; (**B**) UV-C radiation, at 10 min of treatment.

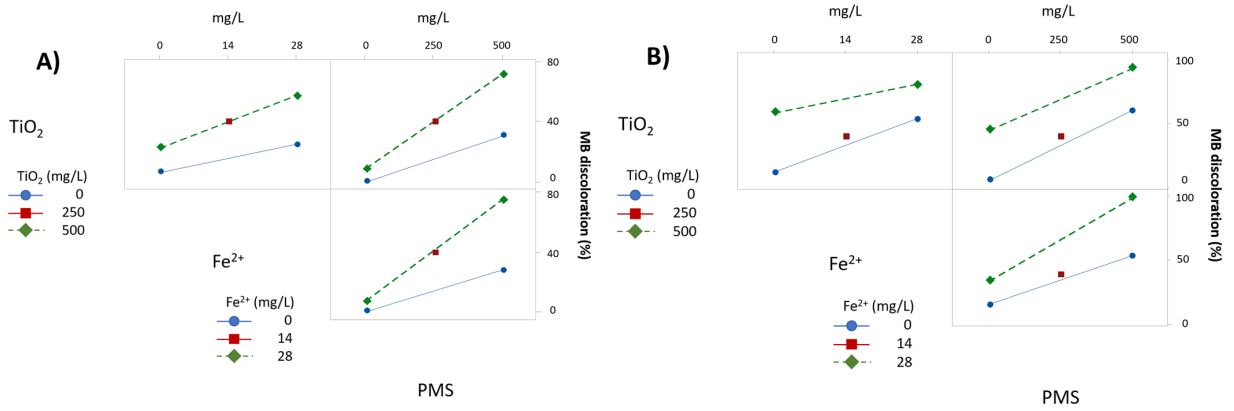

Figure 7. Interaction of variables plot under (**A**) UV-A radiation; (**B**) UV-C radiation, at 5 min of treatment.

Finally, the significance and importance of the variables and their interactions are graphically represented in the Pareto chart (Figure 8), and with *p*-values form the ANOVA (Table S1, Supplementary Material). Additionally, the magnitude of the effects are shown in Table S2 (Supplementary Material). ANOVA analysis was performed to confirm with certainty the effect of a combination of several factors for PMS activation on MB removal.

As can be observed in Figure 8, the lower energetic content of UV-A radiation increases the importance of variables (PMS, TiO_2 or Fe^{2+}), but also, all factors and their interactions subjected to UV-A radiation were significant considering a significance level (α) of 0.05. However, UV-C radiation performed resulted in higher discoloration rates, as shown in Figure 7B. For the main effects, the reduction in the importance of the variables is likely a consequence of the high discoloration yield that can be obtained with the additive effect of UV-C radiation in the absence of the other variables, particularly the experiments where the interaction of Fe^{2+} and TiO_2 does not have a significant effect (Table S1, Supplementary Material).

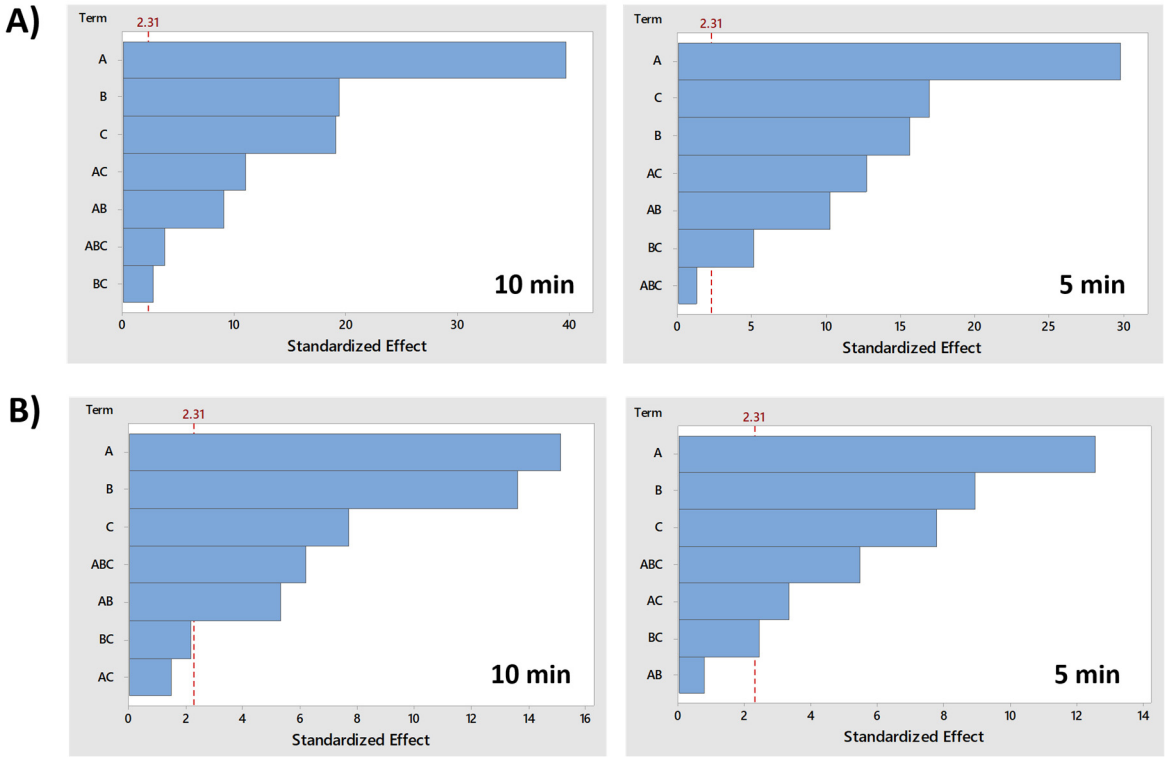

Figure 8. Pareto chart of standardized effects ($\alpha = 0.05$) for MB discoloration after 10 and 5 min under (**A**) UV-A radiation; (**B**) UV-C radiation. Factor names: A = PMS; B = TiO_2; C = Fe^{2+}.

As observed in Figure 8, individual factors are of greatest importance in combination with UV radiation (UV-A and UV-C), but with some differences. For example, all factors and their interactions are significant in UV-A spectra, and the factor that showed the highest impact (measured as the size of the effect) was PMS but with minor differences compared with the TiO_2 effect. In contrast, UV-C radiation has shown that, although both are very significant, the TiO_2 effect was half the effect of PMS. In addition, in both cases, Fe^{2+} had a high importance in MB discoloration. The three factors greatly contributed to the degradation of the organic molecule by additive effects, even more than the interaction effects.

However, the most important information that can be extracted from the Pareto chart is related to the importance of interactions, especially those that help to understand the catalysis or activation of PMS by TiO_2 or Fe^{2+}. Regarding the aforementioned, under UV-A radiation (Figure 7A), the combination between PMS and TiO_2 (AB interaction) is considered significant, although the response is slightly lower than the combination of PMS with Fe^{2+} (AC interaction). However, although the AB interaction is considered significant and contributed to the increase of the response factor (MB discoloration), most organic degradation occurs not by the interaction, but by the additive effects of the individual factor (PMS, TiO_2). In any case, the combination of both substances has a positive effect on the response factor, increasing the MB discoloration.

The results are totally different under UV-C radiation (Figure 7B). In this case, the interaction of AB (PMS/TiO_2) is considered also significant, but the magnitudes of the effects are negative, indicating that the interaction effect reduces the degradation of the organic molecule and that the high elimination yield of both factors acting together is achieved by the individual additive effects and the effect exerted by UV-C radiation, but not by the catalysis.

Similar results were observed for the AC interaction (PMS/Fe^{2+}) when subjected to UV-C radiation. However, this does not mean that there is no activation or synergy between PMS and Fe^{2+} or that the interaction reduces degradation. In fact, the results for the AC experiment at 10 min showed total degradation of MB. Therefore, the probability that the

maximum degradation rate was achieved before the 10-min sampling period causing and underestimating the multiplicative effect of the interaction when compared with additive effects of the variables should be considered. ANOVA cannot evaluate differences between additive effects of the individual factors and the multiplicative effect of the interaction. Considering this, a 5-min sampling ANOVA was conducted to determine whether there was a positive interaction effect. The results showed that there is, in fact, a significant and positive interaction that increases PMS activation, enhancing the degradation of the organic molecule. The main hypothesis is, again, related with the high energy of UV-C radiation that can individually affect the response factor, leading to high levels of MB discoloration.

Taking into account these results, different conclusions can be drawn. First, it can be concluded that the interaction of PMS and Fe^{2+} is significant in combination with UV-A and UV-C radiation; additionally, the additive effects of individual factors contribute more than the activation of PMS by Fe^{2+}. Regarding the PMS/TiO_2 combination, the *p*-value for the interaction under UV-A radiation was less than the level of significance of 0.05, so it was considered significant, and the probability of a multiplicative effect increasing the elimination of MB should not be discarded. The effect exerted by the interaction subjected to UV-C radiation is also significant with a *p*-value less than 0.05.

Finally, the analysis of variance on the effect of the interaction between the three factors (PMS/Fe^{2+}/TiO_2) when they were subjected to UV-A radiation at 10 min shows that the probability that the MB removal performance increased or decreased when the three factors were at the high level is significant. However, since the experiment achieved the maximum degradation rates before 10 min, and the ANOVA at 5-min sampling showed that there was not a significant interaction, a not-significant effect should be considered. The high removal rates were probably achieved by the additive effects of the factorial interactions, plus individual factor effects, but not by an interaction of the three factors.

Similar conclusions are reached under UV-C radiation. The result of the *p*-value at 5 min was significant, but the numeric regression showed it was negative, which means that the interaction does not contribute to enhance degradation of the organic molecule. The high removal performance of this experiment is achieved by the additive effects of every factor and the tow factor interactions.

4. Conclusions

From a statistical point of view, TiO_2 photocatalysis increases as the wavelength of UV radiation decreases, but PMS/Fe^{2+} contributes more to the elimination rates when subjected to UV-A radiation. Additionally, the greatest contribution in elimination is obtained from the variables itself, and not by their interactions. Regarding ANOVA, experiments using only PMS, Fe^{2+}, or TiO_2 were all significant when subjected to both UV-A and UV-C, meaning that activation of PMS by UV radiation contributes in a relevant way to dye degradation, but also that the other variables (Fe^{2+} and TiO_2) have an important contribution to elimination rates.

Furthermore, the results indicate that there is a significant interaction when using PMS with Fe^{2+} in both UV-A and UV-C radiation. The multiplicative effect of the interaction likely produced by sulfate radicals contributes to the elimination with a high certainty.

The interaction of PMS/TiO_2 is similar to that of the PMS/Fe^{2+} interaction, where UV-A radiation experiments were significant and the interaction was positive, meaning it contributes to elimination. However, experiments subjected to UV-C radiation show that there is an interaction between these variables, but with a negative effect, meaning that it does not contribute to the increase in elimination rates and that the observed high elimination rates are achieved by the oxidation potential of UV-C, and the effect of PMS and TiO_2 by itself.

Supplementary Materials: The following are available online at https://www.mdpi.com/article/10.3390/w13202860/s1, Table S1: Analysis of variance (ANOVA) for the different factor combination (PMS, Fe^{2+} and TiO_2). The degrees of freedom used (df), the sum of squares, the mean square and the F and p values are shown, Table S2: Standardised effects for the different factor combination (PMS,

Fe^{2+} and TiO_2). Estimated numerical regression effects, regression coefficients, standard error (SE), standardised effects (t-value) and *p*-value, for student's *t*-test, are shown.

Author Contributions: Conceptualization, J.M.d.A. and J.R.-C.; methodology, R.G.-Q., J.M.d.A., J.R.-C.; software, R.G.-Q.; validation, J.M.d.A., J.R.-C.; formal analysis, R.G.-Q., J.M.d.A., J.R.-C.; investigation, R.G.-Q.; resources, J.R.-C.; data curation, R.G.-Q.; writing—original draft preparation, R.G.-Q.; writing—review and editing, R.G.-Q., J.M.d.A., J.R.-C.; supervision, J.M.d.A., J.R.-C.; project administration, J.R.-C.; funding acquisition, J.R.-C. All authors have read and agreed to the published version of the manuscript.

Funding: This research was funded by the Community of Madrid (Comunidad de Madrid) for funding the research project IN_REUSE (APOYO-JOVENES-X5PKL6-88-KZ46KU) within the framework of the multi-year agreement with the Universidad Politécnica de Madrid.

Institutional Review Board Statement: Not applicable.

Informed Consent Statement: Not applicable.

Acknowledgments: Jorge Rodríguez-Chueca acknowledges the Community of Madrid (Comunidad de Madrid) for funding the research project IN_REUSE (APOYO-JOVENES-X5PKL6-88-KZ46KU) within the framework of the multi-year agreement with the Universidad Politécnica de Madrid.

Conflicts of Interest: The authors declare no conflict of interest.

References

1. Rodríguez-Chueca, J.; Guerra-Rodríguez, S.; Raez, J.M.; López-Muñoz, M.-J.; Rodríguez, E. Assessment of different iron species as activators of $S_2O_8^{2-}$ and HSO_5^- for inactivation of wild bacteria strains. *Appl. Catal. B Environ.* **2019**, *248*, 54–61. [CrossRef]
2. Chueca, J.J.R.; Ormad, M.P.; Mosteo, R.; Canalis, S.; Ovelleiro, J.L. *Escherichia coli* Inactivation in Fresh Water Through Photocatalysis with TiO_2-Effect of H_2O_2 on Disinfection Kinetics. *CLEAN–Soil Air Water* **2016**, *44*, 515–524. [CrossRef]
3. Pueyo, N.; Rodríguez-Chueca, J.; Ovelleiro, J.L.; Ormad, M.P. Limitations of the Removal of Cyanide from Coking Wastewater by Treatment with Hydrogen Peroxide. *Water Air Soil Pollut.* **2016**, *227*, 1–10. [CrossRef]
4. Rodríguez-Chueca, J.; Mediano, A.; Pueyo, N.; García-Suescun, I.; Mosteo, R.; Ormad, M.P. Degradation of chloroform by Fenton-like treatment induced by electromagnetic fields: A case of study. *Chem. Eng. Sci.* **2016**, *156*, 89–96. [CrossRef]
5. Ghanbari, F.; Giannakis, S.; Lin, K.-Y.A.; Wu, J.; Madihi-Bidgoli, S. Acetaminophen degradation by a synergistic peracetic acid/UVC-LED/Fe(II) advanced oxidation process: Kinetic assessment, process feasibility and mechanistic considerations. *Chemosphere* **2020**, *263*, 128119. [CrossRef]
6. Casado, C.; Moreno-SanSegundo, J.; De la Obra, I.; García, B.E.; Pérez, J.A.S.; Marugán, J. Mechanistic modelling of wastewater disinfection by the photo-Fenton process at circumneutral pH. *Chem. Eng. J.* **2020**, *403*, 126335. [CrossRef]
7. Tak, S.; Vellanki, B.P. Comparison of O3-BAC, UV/H2O2-BAC, and O3/H2O2-BAC treatments for limiting the formation of disinfection byproducts during drinking water treatment in India. *J. Environ. Chem. Eng.* **2020**, *8*, 104434. [CrossRef]
8. Liu, M.; Yin, W.; Qian, F.-J.; Zhao, T.-L.; Yao, Q.-Z.; Fu, S.-Q.; Zhou, G.-T. A novel synthesis of porous TiO_2 nanotubes and sequential application to dye contaminant removal and Cr(VI) visible light catalytic reduction. *J. Environ. Chem. Eng.* **2020**, *8*, 104061. [CrossRef]
9. Rodríguez-Chueca, J.; Ferreira, L.C.; Fernandes, J.R.; Tavares, P.B.; Lucas, M.S.; Peres, J.A. Photocatalytic discolouration of Reactive Black 5 by UV-A LEDs and solar radiation. *J. Environ. Chem. Eng.* **2015**, *3*, 2948–2956. [CrossRef]
10. Khan, I.; Saeed, K.; Ali, N.; Khan, I.; Zhang, B.; Sadiq, M. Heterogeneous photodegradation of industrial dyes: An insight to different mechanisms and rate affecting parameters. *J. Environ. Chem. Eng.* **2020**, *8*, 104364. [CrossRef]
11. Rodríguez-Chueca, J.; Garcia-Cañibano, C.; Sarro, M.; Encinas, Á.; Medana, C.; Fabbri, D.; Calza, P.; Marugán, J. Evaluation of transformation products from chemical oxidation of micropollutants in wastewater by photoassisted generation of sulfate radicals. *Chemosphere* **2019**, *226*, 509–519. [CrossRef] [PubMed]
12. Guerra-Rodríguez, S.; Rodríguez, E.; Singh, D.N.; Rodríguez-Chueca, J. Assessment of Sulfate Radical-Based Advanced Oxidation Processes for Water and Wastewater Treatment: A Review. *Water* **2018**, *10*, 1828. [CrossRef]
13. Wang, J.; Wang, S. Activation of persulfate (PS) and peroxymonosulfate (PMS) and application for the degradation of emerging contaminants. *Chem. Eng. J.* **2018**, *334*, 1502–1517. [CrossRef]
14. Ince, N.; Tezcanli, G.; Belen, R.; Apikyan, I. Ultrasound as a catalyzer of aqueous reaction systems: The state of the art and environmental applications. *Appl. Catal. B Environ.* **2001**, *29*, 167–176. [CrossRef]
15. Ghanbari, F.; Moradi, M. Application of peroxymonosulfate and its activation methods for degradation of environmental organic pollutants: Review. *Chem. Eng. J.* **2017**, *310*, 41–62. [CrossRef]
16. Marjanovic, M.; Giannakis, S.; Grandjean, D.; de Alencastro, L.F.; Pulgarin, C. Effect of μM Fe addition, mild heat and solar UV on sulfate radical-mediated inactivation of bacteria, viruses, and micropollutant degradation in water. *Water Res.* **2018**, *140*, 220–231. [CrossRef] [PubMed]

17. Xiao, S.; Cheng, M.; Zhong, H.; Liu, Z.; Liu, Y.; Yang, X.; Liang, Q. Iron-mediated activation of persulfate and peroxymonosulfate in both homogeneous and heterogeneous ways: A review. *Chem. Eng. J.* **2019**, *384*, 123265. [CrossRef]
18. Karimian, S.; Moussavi, G.; Fanaei, F.; Mohammadi, S.; Shekoohiyan, S.; Giannakis, S. Shedding light on the catalytic synergies between Fe(II) and PMS in vacuum UV (VUV/Fe/PMS) photoreactors for accelerated elimination of pharmaceuticals: The case of metformin. *Chem. Eng. J.* **2020**, *400*, 125896. [CrossRef]
19. Chueca, J.J.R.; Amor, C.; Mota, J.; Lucas, M.S.; Peres, J. Oxidation of winery wastewater by sulphate radicals: Catalytic and solar photocatalytic activations. *Environ. Sci. Pollut. Res.* **2017**, *24*, 22414–22426. [CrossRef] [PubMed]
20. Moreno-Andrés, J.; Farinango, G.; Romero-Martínez, L.; Acevedo-Merino, A.; Nebot, E. Application of persulfate salts for enhancing UV disinfection in marine waters. *Water Res.* **2019**, *163*, 114866. [CrossRef]
21. Solís, R.R.; Rivas, F.J.; Chávez, A.M.; Dionysiou, D.D. Peroxymonosulfate/solar radiation process for the removal of aqueous microcontaminants. Kinetic modeling, influence of variables and matrix constituents. *J. Hazard. Mater.* **2020**, *400*, 123118. [CrossRef] [PubMed]
22. Verma, S.; Nakamura, S.; Sillanpää, M. Application of UV-C LED activated PMS for the degradation of anatoxin-a. *Chem. Eng. J.* **2016**, *284*, 122–129. [CrossRef]
23. Sharma, J.; Mishra, I.M.; Dionysiou, D.D.; Kumar, V. Oxidative removal of Bisphenol A by UV-C/peroxymonosulfate (PMS): Kinetics, influence of co-existing chemicals and degradation pathway. *Chem. Eng. J.* **2015**, *276*, 193–204. [CrossRef]
24. Rodríguez-Chueca, J.; Silva, T.; Fernandes, J.R.; Lucas, M.S.; Puma, G.L.; Peres, J.A.; Sampaio, A. Inactivation of pathogenic microorganisms in freshwater using HSO_5^-/UV-A LED and HSO_5^-/M^{n+}/UV-A LED oxidation processes. *Water Res.* **2017**, *123*, 113–123. [CrossRef]
25. Zhang, J.; Song, H.; Liu, Y.; Wang, L.; Li, D.; Liu, C.; Gong, M.; Zhang, Z.; Yang, T.; Ma, J. Remarkable enhancement of a photochemical Fenton-like system (UV-A/Fe(II)/PMS) at near-neutral pH and low Fe(II)/peroxymonosulfate ratio by three alpha hydroxy acids: Mechanisms and influencing factors. *Sep. Purif. Technol.* **2019**, *224*, 142–151. [CrossRef]
26. Anipsitakis, G.P.; Tufano, T.P.; Dionysiou, D.D. Chemical and microbial decontamination of pool water using activated potassium peroxymonosulfate. *Water Res.* **2008**, *42*, 2899–2910. [CrossRef]
27. Anipsitakis, G.P.; Dionysiou, D.D. Radical Generation by the Interaction of Transition Metals with Common Oxidants. *Environ. Sci. Technol.* **2004**, *38*, 3705–3712. [CrossRef] [PubMed]
28. Rodríguez-Chueca, J.; Amor, C.; Silva, T.; Dionysiou, D.D.; Puma, G.L.; Lucas, M.S.; Peres, J.A. Treatment of winery wastewater by sulphate radicals: HSO_5^-/transition metal/UV-A LEDs. *Chem. Eng. J.* **2017**, *310*, 473–483. [CrossRef]
29. Rodríguez-Chueca, J.; Barahona-García, E.; Blanco-Gutiérrez, V.; Isidoro-García, L.; Dos Santos-García, A. Magnetic $CoFe_2O_4$ ferrite for peroxymonosulfate activation for disinfection of wastewater. *Chem. Eng. J.* **2020**, *398*, 125606. [CrossRef]
30. Rodríguez-Chueca, J.; Alonso, E.; Singh, D.N. Photocatalytic Mechanisms for Peroxymonosulfate Activation through the Removal of Methylene Blue: A Case Study. *Int. J. Environ. Res. Public Health* **2019**, *16*, 198. [CrossRef]
31. Xu, B.; Ahmed, M.B.; Zhou, J.L.; Altaee, A. Visible and UV photocatalysis of aqueous perfluorooctanoic acid by TiO2 and peroxymonosulfate: Process kinetics and mechanistic insights. *Chemosphere* **2019**, *243*, 125366. [CrossRef] [PubMed]
32. Jia, J.; Liu, D.; Wang, S.; Li, H.; Ni, J.; Li, X.; Tian, J.; Wang, Q. Visible-light-induced activation of peroxymonosulfate by TiO_2 nano-tubes arrays for enhanced degradation of bisphenol A. *Sep. Purif. Technol.* **2020**, *253*, 117510. [CrossRef]
33. Zhao, Y.; Wang, G.; Li, L.; Dong, X.; Zhang, X. Enhanced activation of peroxymonosulfate by nitrogen-doped graphene/TiO_2 under photo-assistance for organic pollutants degradation: Insight into N doping mechanism. *Chemosphere* **2019**, *244*, 125526. [CrossRef]
34. Nengzi, L.-C.; Yang, H.; Hu, J.-Z.; Zhang, W.-M.; Jiang, D.-A. Fabrication of SnS/TiO2 NRs/NSs photoelectrode as photoactivator of peroxymonosulfate for organic pollutants elimination. *Sep. Purif. Technol.* **2020**, *249*, 117172. [CrossRef]
35. Chen, X.; Wang, W.; Xiao, H.; Hong, C.; Zhu, F.; Yao, Y.; Xue, Z. Accelerated TiO2 photocatalytic degradation of Acid Orange 7 under visible light mediated by peroxymonosulfate. *Chem. Eng. J.* **2012**, *193–194*, 290–295. [CrossRef]
36. Zazouli, M.A.; Ghanbari, F.; Yousefi, M.; Madihi-Bidgoli, S. Photocatalytic degradation of food dye by Fe3O4–TiO2 nanoparticles in presence of peroxymonosulfate: The effect of UV sources. *J. Environ. Chem. Eng.* **2017**, *5*, 2459–2468. [CrossRef]
37. Shaham-Waldmann, N.; Paz, Y. Away from TiO 2: A critical minireview on the developing of new photocatalysts for degradation of contaminants in water. *Mater. Sci. Semicond. Process.* **2016**, *42*, 72–80. [CrossRef]
38. Bianchi, C.; Colombo, E.; Gatto, S.; Stucchi, M.; Cerrato, G.; Morandi, S.; Capucci, V. Photocatalytic degradation of dyes in water with micro-sized TiO_2 as powder or coated on porcelain-grès tiles. *J. Photochem. Photobiol. A: Chem.* **2014**, *280*, 27–31. [CrossRef]
39. Ling, L.; Zhang, D.; Fan, C.; Shang, C. A Fe(II)/citrate/UV/PMS process for carbamazepine degradation at a very low Fe(II)/PMS ratio and neutral pH: The mechanisms. *Water Res.* **2017**, *124*, 446–453. [CrossRef]
40. Tan, C.; Dong, Y.; Shi, L.; Chen, Q.; Yang, S.; Liu, X.; Ling, J.; He, X.; Fu, D. Degradation of Orange II in ferrous activated peroxymonosulfate system: Efficiency, situ EPR spin trapping and degradation pathway study. *J. Taiwan Inst. Chem. Eng.* **2018**, *83*, 74–81. [CrossRef]
41. Rao, Y.; Xue, D.; Pan, H.; Feng, J.; Li, Y. Degradation of ibuprofen by a synergistic UV/Fe(III)/Oxone process. *Chem. Eng. J.* **2016**, *283*, 65–75. [CrossRef]
42. Zeng, X.; Chen, J.; Qu, R.; Feng, M.; Wang, Z. Degradation of octafluorodibenzo-pdioxin by UV/Fe(II)/potassium monopersulfate system: Kinetics, influence of coexisting chemicals, degradation products and pathways. *Chem. Eng. J.* **2017**, *319*, 98–107. [CrossRef]

43. Rastogi, A.; Al-Abed, S.R.; Dionysiou, D.D. Sulfate radical-based ferrous–peroxymonosulfate oxidative system for PCBs degradation in aqueous and sediment systems. *Appl. Catal. B Environ.* **2009**, *85*, 171–179. [CrossRef]
44. Durango-Usuga, P.; Guzmán-Duque, F.; Mosteo, R.; Vazquez, M.V.; Peñuela, G.; Torres-Palma, R.A. Experimental design approach applied to the elimination of crystal violet in water by electrocoagulation with Fe or Al electrodes. *J. Hazard. Mater.* **2010**, *179*, 120–126. [CrossRef] [PubMed]
45. Rodriguez, S.; Vasquez, L.; Costa, D.; Romero, A.; Santos, A. Oxidation of Orange G by persulfate activated by Fe(II), Fe(III) and zero valent iron (ZVI). *Chemosphere* **2014**, *101*, 86–92. [CrossRef] [PubMed]
46. Andrade, G.R.; Nascimento, C.C.; Júnior, E.C.S.; Mendes, D.T.; Gimenez, I. ZnO/Au nanocatalysts for enhanced decolorization of an azo dye under solar, UV-A and dark conditions. *J. Alloy. Compd.* **2017**, *710*, 557–566. [CrossRef]
47. Monteagudo, J.M.; Durán, A.; Martín, I.S.; Acevedo, A.M. A novel combined solar pasteurizer/TiO_2 continuous-flow reactor for decontamination and disinfection of drinking water. *Chemosphere* **2017**, *168*, 1447–1456. [CrossRef]
48. Tichapondwa, S.; Newman, J.; Kubheka, O. Effect of TiO_2 phase on the photocatalytic degradation of methylene blue dye. *Phys. Chem. Earth Parts A/B/C* **2020**, *118–119*, 102900. [CrossRef]
49. Yao, H.; Pei, J.; Wang, H.; Fu, J. Effect of Fe(II/III) on tetracycline degradation under UV/VUV irradiation. *Chem. Eng. J.* **2017**, *308*, 193–201. [CrossRef]
50. Wu, S.; Li, H.; Li, X.; He, H.; Yang, C. Performances and mechanisms of efficient degradation of atrazine using peroxymonosulfate and ferrate as oxidants. *Chem. Eng. J.* **2018**, *353*, 533–541. [CrossRef]
51. Jiao, Y.; Shang, H.; Scott, J.A. A UVC based advanced photooxidation reactor design for remote households and communities not connected to a municipal drinking water system. *J. Environ. Chem. Eng.* **2021**, *9*, 105162. [CrossRef]